Available online at www.sciencedirect.com
SCIENCE DIRECT®
Journal of Solid State Chemistry 172 (2003) 22–26
JOURNAL OF SOLID STATE CHEMISTRY
http://elsevier.com/locate/jssc

Single-crystal growth, crystal and electronic structure of $NaCoO_2$

Yasuhiko Takahashi,[a,b,*] Yoshito Gotoh,[a] and Junji Akimoto[a]

[a] National Institute of Advanced Industrial Science and Technology (AIST), 1-1-1 Higashi, Tsukuba, Ibaraki 305-8565, Japan
[b] Japan Society for the Promotion of Science, 6 Ichibancho, Chiyoda-ku, Tokyo 102-8471, Japan

Received 13 May 2002; received in revised form 3 September 2002; accepted 12 September 2002

Abstract

Single crystals of $NaCoO_2$ have been successfully synthesized for the first time by a flux method at 1323 K. A single-crystal X-ray diffraction study confirmed the trigonal $R\bar{3}m$ space group and the lattice parameters $a = 2.8897(15)$ Å, $c = 15.609(3)$ Å. The crystal structure has been refined to the conventional values $R = 1.9\%$ and $wR = 2.1\%$ for 309 independent observed reflections. The electron density distribution of $NaCoO_2$ has been studied by the maximum entropy method (MEM) using single-crystal X-ray diffraction data obtained at 298 K. From the results of the MEM analysis, the strong covalent bonding was clearly observed between Co and O atoms, while no bonding was observed around Na atoms. We also calculated the electron density of $NaCoO_2$ by first principles calculations. The electron density obtained experimentally is in good agreement with the theoretical one.

Keywords: Thermo electric oxide; Single-crystal growth; X-ray diffraction; Crystal structure; Electronic structure

1. Introduction

Transition metal oxides with the layered AMO_2 (A: Alkali, M: Metal) structure have been widely studied. In these materials, $LiCoO_2$ is used industrially as a cathode material for lithium-ion rechargeable batteries [1]. The crystal structure of $NaCoO_2$ was originally reported by Fouassier et al. [2] and Jansen et al. [3]. They determined the crystal structure using powder diffraction data. Delmas et al. reported that the non-stoichiometric Na_xCoO_2 compounds were metallic, while stoichiometric $NaCoO_2$ was a semiconductor [4]. Recently, Terasaki et al. discovered that $NaCo_2O_4$ single crystal was a potential thermoelectric material because of the large thermoelectric power and low resistivity [5].

To clarify the physical and chemical properties, it is important to understand precise chemical bonding nature in detail. The accurate single-crystal X-ray diffraction study is one of the most indispensable methods to understand the nature as well as thermal displacement of atoms in materials precisely. Furthermore, the maximum entropy method (MEM) has been found to be efficient in determining electron density distribution in crystalline materials [6–8].

In the present study, we report the synthesis of $NaCoO_2$ single crystal by a flux method, the X-ray structure refinement of the single crystal of $NaCoO_2$ for the first time, and the electron density distributions analyzed by the MEM. The obtained electron density distributions are compared with the theoretically ones calculated by the first principles full-potential linearized augmented-plane-wave (FLAPW) method for understanding the nature of chemical bonding.

2. Experimental

Single crystals of $NaCoO_2$ were synthesized by a flux method. A Co_3O_4 (99.9%) powder was mixed with Na_2CO_3 (99%) and NaCl (99.9%) powder to form flux material in the nominal weight ratio of Co_3O_4:Na_2CO_3:NaCl = 1:5:5. The flux growth was conducted in a resistance furnace. The mixture was heated to 1323 K for 10 h in an Al_2O_3 crucible in air and gradually cooled to 1123 K at a rate of 5 K/h. The products were separated mechanically from the frozen flux without washing with water. The crystals thus obtained were checked by SEM-EDX (JEOL JSM-5400) analysis. Chemical analysis showed that the crystals were free from aluminum impurity from the crucible and the ratio

*Corresponding author. Fax: +81-298-61-4555.
E-mail address: yas-takahashi@aist.go.jp (Y. Takahashi).

0022-4596/03/$ - see front matter © 2002 Elsevier Science (USA). All rights reserved.
doi:10.1016/S0022-4596(02)00042-7

of Na/Co was equal to 1.0. A typical crystal shape obtained was a hexagonal platelet of about $0.5 \times 0.5 \times 0.02\,mm^3$ in size, as shown in Fig. 1. A small hexagonal platelet crystal, $0.14 \times 0.14 \times 0.01\,mm^3$ in size, was used for the X-ray intensity data collection. To protect the specimen from humidity, it was coated with adhesive.

The intensity data were collected in the 2θ-ω scan mode at a scan rate of 1.0°/min. at 298 K on a four-circle diffractometer (Rigaku AFC-5S, operating conditions: 45 kV, 35 mA) using graphite-monochromatized Mo$K\alpha$ radiation ($\lambda = 0.71073$ Å). A total of 2644 reflections were measured within the limit of $2\theta < 135°$ ($\sin\theta/\lambda < 1.3$ Å^{-1}), and the averaged 309 independent reflections were used for the structure refinement. The standard reflections taken after every 150 observations were monitored and the fluctuation of intensities was within 1.0%. The lattice parameters, determined by least-square fitting using 25 strong reflections in the 2θ range of 31.1–34.7°, were $a = 2.8897(15)$ Å, $c = 15.609(3)$ Å, and $c/a = 5.402(5)$. These values agree well with the reported powder data for $NaCoO_2$ [2,3]. The experimental summaries for the present $NaCoO_2$ single crystal are given in Table 1.

Table 1
The experimental and crystallographic summaries for $NaCoO_2$ single crystal

X-ray wavelength (Å)	0.71073 (Mo$K\alpha$)
Temperature (K)	298
Crystal system	Trigonal
Space group	$R\bar{3}m$
Lattice parameters	
a (Å)	2.8897(15)
c (Å)	15.609(3)
V (Å^3)	112.88(12)
Z	3
D_x (g/cm^3)	5.028
Crystal size (mm)	$0.14 \times 0.14 \times 0.01$
hkl range	$-7 \leqslant h$, $k \leqslant 7$, $-40 \leqslant l \leqslant 40$
Maximum 2θ (deg)	135
Scan method	$2\theta-\omega$
Scan speed (deg/min.)	1
Absorption correction	Gaussian integration
Transmission factors	
Min.	0.242
Max.	0.909
Measured reflections	2644
Independent reflections	309
Extinction correction, y_{min}	0.94, (1 0 4)
Number of variables	9
R	0.019
wR[w = $1/\sigma^2 F$]	0.021

3. Result and discussion

3.1. Structure refinement

Structural refinements were carried out using the computer program Xtal3.7 [9]. Structure factors, F_{obs}, were corrected for scale, absorption and isotropic extinction effects [10] after averaging equivalent Bragg intensities. The refined thermal parameters U_{ij} are the mean square displacements of constituent atoms for the ij components. Neutral spherical atomic scattering factors were applied for all atoms in the refinement. In the structure analysis that followed, we adopted the space group of highest symmetry, $R\bar{3}m$, which was confirmed by successful refinement.

At the final stage of refinement, site-population refinements were applied using three models as follows: (I) the 100% Na, Co and O occupation model at the 3a, 3b and 6c sites, respectively, (II) the Na-deficiency model at the 3a site, (III) the O-deficiency model at the 6c site. Model (II) did not improve the R-value with the resultant Na population value of 0.997(7). Model (III) also did not improve the R-value with the O population value of 1.003(7). Therefore, these results clearly indicated that model (I) was most reliable in this study.

Finally, the structure parameters at 298 K were refined to $R = 0.019$ and w$R = 0.021$ for 309 independent reflections, with a shift/error for all nine parameters of less than 0.001. Detailed structure refinement parameters are shown in Table 2. The structure thus refined is basically the same as that in the previous report [3]. However the present results provide a more precise structure of $NaCoO_2$.

The Co–O distance of 1.9411(8) Å and the short O–O′ distance of 2.5924(10) Å in $NaCoO_2$ are similar to those in $LiCoO_2$ [11], the values of which are 1.9213(12) and 2.614(2) Å, respectively. This fact suggests that the coordination environment of the CoO_6 octahedron in $NaCoO_2$ is very similar with that in $LiCoO_2$. On the other hand, the Na–O distance of 2.3181(8) Å is longer

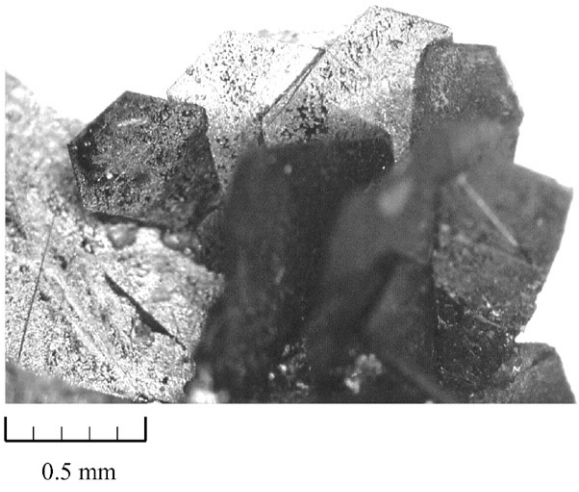

Fig. 1. The photograph of hexagonal platelet $NaCoO_2$ single crystals (1 grid unit = 0.1 mm).

Table 2
Final structural parameters, selected bond distances and angles for $NaCoO_2$

U_{eq} (Å^2) for Na atom	0.0074(2)
U_{11} (Å^2)	0.0075(2)
U_{33} (Å^2)	0.0074(2)
U_{eq} (Å^2) for Co atom	0.00311(5)
U_{11} (Å^2)	0.00259(5)
U_{33} (Å^2)	0.00417(5)
z for O atom at (0, 0, z)	0.23023(5)
U_{eq} (Å^2) for O atom	0.0046(1)
U_{11} (Å^2)	0.0042(1)
U_{33} (Å^2)	0.0055(1)
CoO_6 octahedron	
Co–O distance (Å)	1.9411(8)
O–O′ (Å)	2.5924(10)
O–O (Å)	2.8897(15)
O–Co–O′ angle (°)	83.79(34)
O–Co–O (°)	96.21(3)
NaO_6 octahedron	
Na–O distance (Å)	2.3181(8)
O–O′ (Å)	3.6254(11)
O–O (Å)	2.8897(15)
O–Na–O′ angle (°)	102.89(3)
O–Na–O (°)	77.12(3)

Atomic coordinates are Na at the $3a(0,0,0)$, Co at the $3b(0,0,1/2)$, O at the $6c(0,0,z)$ positions, respectively. Temperature parameter conditions are $U_{11}=U_{22}=2U_{12}$ and $U_{13}=U_{23}$, respectively. The anisotropic thermal parameters are defined as $\exp\left\{-2\pi^2\sum_{ij}h_ih_ja_i^*a_j^*U_{ij}\right\}$.

than the Li–O distance of 2.0934(14) Å in $LiCoO_2$. This can be explained by the difference of the size between Na and Li ions. The present Na–O distance is normal for the NaO_6 octahedral coordination, e.g., 2.353 Å in the isostructural $NaCrO_2$ reported by Scheld and Hoppe [12]. The refined anisotropic temperature parameters of U_{11} and U_{33} for Na atom in $NaCoO_2$ are 0.0075(2) and 0.0074(2) Å^2, respectively, indicating an isotropic characteristic.

3.2. Electron density obtained by the MEM

To obtain the electron density in $NaCoO_2$, the MEM analysis was carried out with the computer program MEED [13]. In the present analysis, total electrons in the unit cell were fixed to be $F(0\,0\,0)$ (162 e for $NaCoO_2$) and the unit cell was divided into $100\times100\times500$ pixels to ensure good spatial resolution. A total of 309 independent reflections in the range of $\sin\theta/\lambda<1.3$ Å^{-1} were used. The reliability factor of the MEM, R_{MEM}, was 1.12%. R_{MEM} is expressed as $R_{MEM}=\sum|F_{obs}-F_{MEM}|/\sum|F_{obs}|$, where F_{obs} is obtained by structural refinement and F_{MEM} the structure factor calculated from electron density obtained by the MEM.

Figs. 2a and b show the electron density, $\rho(r)_{obs}$, in $NaCoO_2$ at 298 K on $(2\bar{1}0)$ and (100) plane, respectively. The contour lines are drawn from 0.15 to 4.15 e/Å^3 with 0.1 e/Å^3 intervals. Strong covalent bonding is clearly visible between Co and O atoms, while no bonding is observed between Na and O atoms. The electron density height at the saddle point between Co and O atoms is analyzed to be 0.81 e/Å^3. On the contrary, the Na–O (0.21 e/Å^3), Na–Na (0.07 e/Å^3), Co–Co (0.24 e/Å^3), O–O′ (0.23 e/Å^3) and O–O (0.16 e/Å^3) bonds are found to be weaker than the Co–O bonding, from the viewpoint of bonding electron at the saddle points. It is considered that the covalent bonding of Co–O is on account of Co-3d and O-2p interaction near the Fermi level.

To analyze the spatial anisotropy of the electron density distribution, we carried out the subtraction of the MEM electron density of $\rho(r)_{obs}$ directly from those of $\rho(r)_{calc}$. The $\rho(r)_{calc}$ was obtained from the MEM analysis using calculated structure factors F_{calc}, and corresponded to spherical electron density of atoms. Fig. 3 shows the difference electron density, $\Delta\rho(r)_{MEM}=\rho(r)_{obs}-\rho(r)_{calc}$, on the magnified $(2\bar{1}0)$ plane. The contour lines are drawn from −3.0 to 3.0 e/Å^3 with 0.15 e/Å^3 intervals. Solid (red) and dotted (blue) lines are shown with positive and negative parts, respectively. The spatial anisotropy in electron density is clearly observed around the Co atom. Negative regions around the Co atom are found along the neighboring O atom direction, while positive regions avoiding the O atom direction. To understand these results from a theoretical point of view, we calculated electron density distribution of $NaCoO_2$ by first principles calculations.

3.3. Electron density obtained by the flapw calculations

Aydinol et al. reported detailed first-principles band calculations in lithium transition metal oxides [14]. They

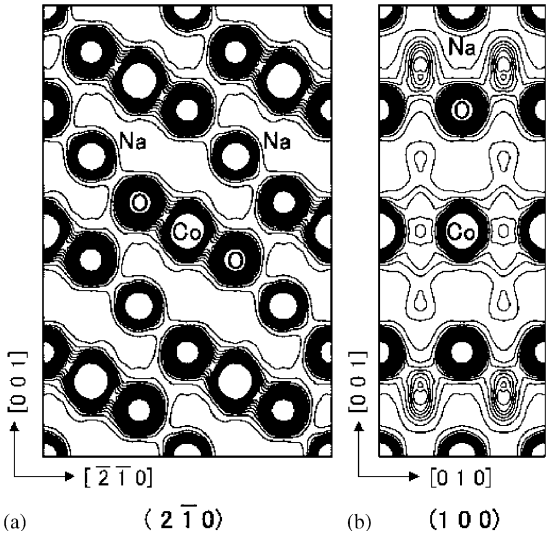

Fig. 2. The electron density in $NaCoO_2$ at 298 K on (a) $(2\bar{1}0)$ and (b) (100) plane obtained by the MEM. Contours are drawn from 0.15 to 4.15 e/Å^3 with 0.1 e/Å^3 intervals.

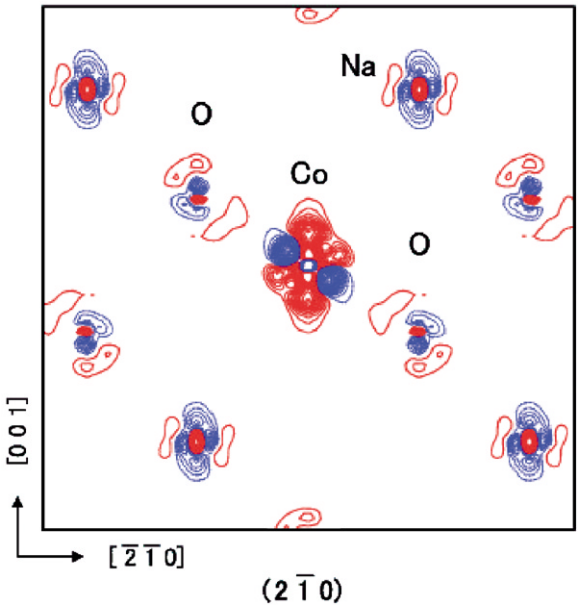

Fig. 3. The difference electron density, $\Delta\rho(r)_{MEM}=\rho(r)_{obs}-\rho(r)_{calc}$, was shown on the magnified $(2\bar{1}0)$ plane. The contour lines are drawn from –3.0 to 3.0 e/Å^3 with 0.15 e/Å^3 intervals. Solid (red) and dotted (blue) lines are shown positive and negative part, respectively.

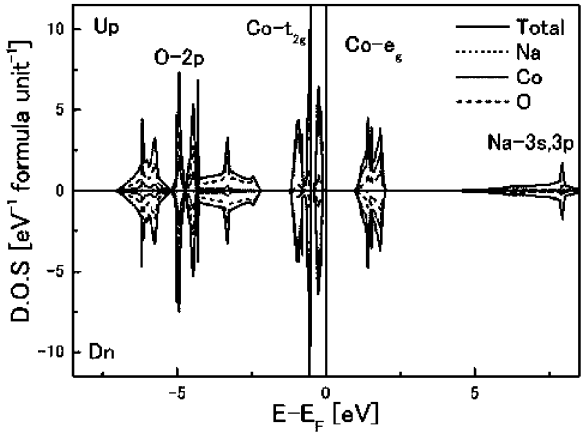

Fig. 4. Total and partial densities of states of $NaCoO_2$ obtained by the FLAPW calculations.

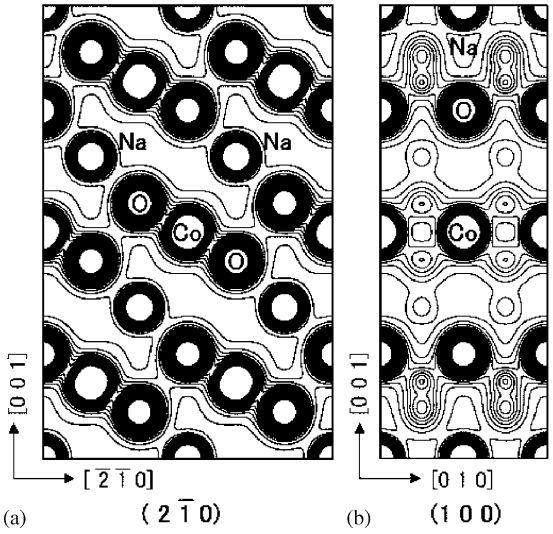

Fig. 5. The electron density in $NaCoO_2$ on (a) $(2\bar{1}0)$ and (b) (100) plane obtained by the FLAPW calculations. Contours are drawn from 0.1 to 4.1 e/Å^3 with 0.1 e/Å^3 intervals.

predicted the average intercalation voltage for Li insertion in various compounds from the viewpoint of applying for the lithium-ion rechargeable battery technology, and concluded that not Co but O redox reaction was important to perform charge and discharge for $LiCoO_2$. On the other hand, Catti calculated detailed electronic structure of $LiCoO_2$ and $Li_{0.5}CoO_2$ by ab initio periodic Hartree–Fock methods with localized atomic-like basis functions and discussed Li diffusion mechanism in the system [15]. Recently, Singh calculated the electronic structure of $NaCo_2O_4$ and discussed the Co-3*d* and O-2*p* electron correlation [16].

In this study, to confirm the electron density obtained by the MEM, we calculated the electronic structure of $NaCoO_2$. The electron density in $NaCoO_2$ was calculated using the full-potential linearized augmented-plane-wave (FLAPW) method with the computer programs WIEN97 package [17]. The exchange and correlation terms of Perdew et al. were employed [18]. Structural parameters were used for trigonal $R\bar{3}m$, lattice parameters $a=2.8897$ Å, $c=15.609$ Å and oxygen coordinate $z=0.23023$ obtained in the present study (Tables 1 and 2). The muffin-tin sphere radii used were 1.7 a.u. (0.90 Å) for Na and 1.9 a.u. (1.01 Å) for Co and 1.6 a.u. (0.85 Å) for O atom, respectively.

Fig. 4 shows total and partial densities of states of $NaCoO_2$ obtained by the FLAPW calculations. The *d* bands of Co consist of t_{2g}- and e_g- type bands. A gap can be seen between the O-2*p* and the Co-3*d* (t_{2g}) bands. A mixture of the O-2*p* bands and the Co-3*d* bands located from −7.0 to −2.0 eV corresponds to the strong covalent bonding between the Co and O atoms. On the other hand, the Na-3*s*, 3*p* states have very small contribution to the O-2*p* bands. This can be accounted for the slight covalent interaction between the Na and O atoms. These features were similar to those in $LiCoO_2$ reported previously [14]. These results suggest that $NaCoO_2$ is a semiconductor and agree with the experimental results [4].

Figs. 5a and b show the electron density distributions in $NaCoO_2$ obtained by the FLAPW calculations on $(2\bar{1}0)$ and (1 0 0) plane, respectively. The contour lines were drawn from 0.1 to 4.1 e/Å^3 with 0.1 e/Å^3 intervals. The covalent bonding is clearly seen between the Co and O atoms and is in good agreement with that obtained by the MEM. In the theoretical calculations, the Co–O bonding is mainly constituted by O-2*p* bands and Co-3*d*

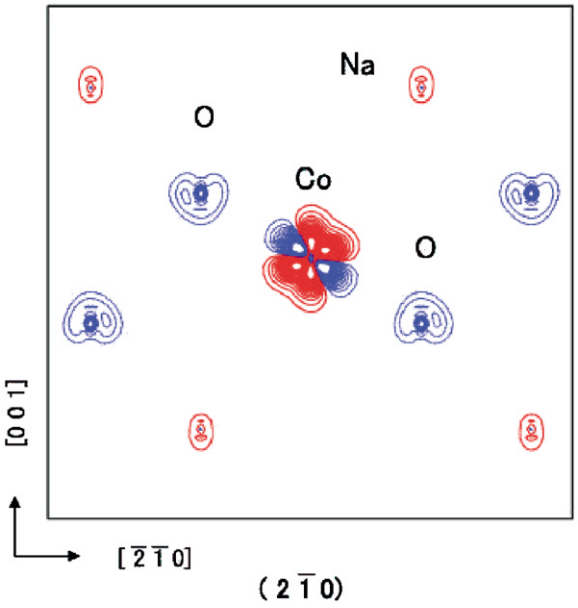

Fig. 6. The difference electron density, $\Delta\rho(r)_{\mathrm{FLAPW}}=\rho(r)_{\mathrm{FLAPW}}-\rho(r)_{\mathrm{atom}}$, was shown on the magnified $(2\bar{1}0)$ plane. Contour lines are drawn from -2.0 to $2.0\,\mathrm{e/\AA^3}$ with $0.1\,\mathrm{e/\AA^3}$ intervals. Solid (red) and dotted (blue) lines are shown positive and negative part, respectively.

bands located from -7.0 to -2.0 eV. The value of the electron density height at saddle point between Co and O is $0.63\ \mathrm{e/\AA^3}$, which is little smaller than the experimental one. Furthermore, Na–O ($0.16\,\mathrm{e/\AA^3}$), Na–Na ($0.04\,\mathrm{e/\AA^3}$), Co–Co ($0.23\,\mathrm{e/\AA^3}$), O–O′ ($0.23\,\mathrm{e/\AA^3}$) and O–O ($0.18\,\mathrm{e/\AA^3}$) bonds are found to be weaker than Co–O bonding. These features are similar to the experimental results.

We carried out the subtraction of the FLAPW electron density of $\rho(r)_{\mathrm{FLAPW}}$ directly from that of $\rho(r)_{\mathrm{atom}}$. The $\rho(r)_{\mathrm{atom}}$ was spherical electron density distribution of atoms and was also calculated by FLAPW calculations. Fig. 6 shows the difference electron density, $\Delta\rho(r)_{\mathrm{FLAPW}}=\rho(r)_{\mathrm{FLAPW}}-\rho(r)_{\mathrm{atom}}$, on the magnified $(2\bar{1}0)$ plane. The contour lines are drawn from -2.0 to $2.0\,\mathrm{e/\AA^3}$ with $0.1\,\mathrm{e/\AA^3}$ intervals. The spatial anisotropy in electron density is clearly observed around the Co atom. This anisotropy could be considered to the Co-3*d* electron density distributions. Negative regions along the O atom directions around the Co atom can be ascribed to Co-3*d* e_g-type anti-bonding electron density distribution located from 0.9 to 2.0 eV.On the other hand, positive regions around the Co atom can be ascribed to Co-3*d* t_{2g}-type non-bonding electron density distribution located from -1.2 to -0.1 eV (Fig. 4). These features are in good agreement with those by the MEM analysis, as shown in Fig. 3.

4. Conclusion

We have succeeded in growing $NaCoO_2$ single crystals for the first time. The structure refinement by single-crystal X-ray diffraction method revealed the precise crystal structure. The nature of chemical bonding in $NaCoO_2$ is understood from the MEM electron density analyses. The strong covalent bonding was observed between Co and O atoms. Furthermore, spatial anisotropy was observed around Co atom, which was assigned to the Co-3*d* electron density distribution. These features are in good agreement with the results by the FLAPW calculations.

References

[1] K. Mizushima, P.C. Jones, P.J. Wiseman, J.B. Goodenough, Mater. Res. Bull. 15 (1980) 783.
[2] C. Fouassier, G. Matejka, J-.M. Reau, P. Hagenmuller, J. Solid State Chem. 6 (1973) 532.
[3] V.M. Jansen, R. Hoppe, Zeit. Anor. Allg. Chem. 408 (1974) 104.
[4] C. Delmas, J.J. Braconnier, C. Fouassier, P. Hagenmuller, Solid State Ionics 3/4 (1981) 165.
[5] I. Terasaki, Y. Sasago, K. Uchinokura, Phys. Rev. B 56 (1997) 12685.
[6] M. Sakata, M. Sato, Acta Crystallogr. A 46 (1990) 263.
[7] M. Takata, E. Nishibori, K. Kato, M. Sakata, Y. Moritomo, J. Phys. Soc. Jpn. 68 (1999) 2190.
[8] M. Takata, E. Nishibori, M. Sakata, M. Inakuma, E. Yamamoto, H. Shinohara, Phys. Rev. Lett. 83 (1999) 2214.
[9] S.R. Hall, D.J. du Boulay,R. Olthof-Hazekamp, (Eds.), Xtal3.7 System, University of Western Australia, Australia, 2000.
[10] W.H. Zachariasen, Acta Crystallogr. 23 (1967) 558.
[11] J. Akimoto, Y. Gotoh, Y. Oosawa, J. Solid State Chem. 141 (1998) 298.
[12] W. Scheld, R. Hoppe, Z. Anorg. Allg. Chem. 568 (1989) 151.
[13] S. Kumazawa, Y. Kubota, M. Takata, M. Sakata, Y. Ishibashi, J. Appl. Cryst. 26 (1993) 453.
[14] M.K. Aydinol, A.F. Kohan, G. Ceder, K. Cho, J. Joannopoulos, Phys. Rev. B 56 (1997) 1354.
[15] M. Catti, Phys. Rev. B 61 (2000) 1795.
[16] D.J. Singh, Phys. Rev. B 61 (2000) 13397.
[17] P. Blaha, K. Schwarz, J. Luitz, WIEN97, A Full Potential Linearized Augmented Plane Wave Package for Calculating Crystal Properties, Karlheinz Schwarz, Techn. Univ. Wien, Vienna, 1999. ISBN3-9501031-0-4 (Updated version of P. Blaha, K. Schwarz, P. Sorantin, and S. B. Trickey, Comp. Phys. Commun. 59 (1990)) 399
[18] P. Perdew, K. Burke, M. Ernzerhof, Phys. Rev. Lett. 77 (1996) 3865.